Hyperfine Interact (2006) 167:839–844
DOI 10.1007/s10751-006-9369-3

Magnetic and thermal Mössbauer effect scans: a new approach

G. A. Pasquevich · P. Mendoza Zélis · F. H. Sánchez · M. B. Fernández van Raap · A. Veiga · N. Martínez

Published online: 8 November 2006

Abstract Mössbauer transmission recorded at fixed photon energies as a function of a given physical parameter such as temperature, external field, etc. (Mössbauer scan), is being developed as a useful quantitative tool, complementary of Mössbauer spectroscopy. Scans are performed at selected energies, suitable for the observation of a given physical property or process. It is shown that one of main advantages of this approach is the higher speed at which the external physical parameter can be swept, which allows the recording of quasi-continuous experimental response functions as well as the study of processes which occur too fast to be followed by Mössbauer spectroscopy. The applications presented here are the determination of the temperature dependence of the ^{57}Fe hyperfine field in $FeSn_2$, the thermal evolution and nanocrystallization kinetics of amorphous $Fe_{73.5}Si_{13.5}Cu_1Nb_3B_9$ and

G. A. Pasquevich · P. Mendoza Zélis · F. H. Sánchez (✉) · M. B. Fernández van Raap · A. Veiga · N. Martínez
Dep. Física, FCE. Universidad Nacional de La Plata, 49 y 115, CC 67, 1900, La Plata, Argentina
e-mail: sanchez@fisica.unlp.edu.ar

G. A. Pasquevich
e-mail: gpasquev@fisica.unlp.edu.ar

P. Mendoza Zélis
e-mail: pmendoza@fisica.unlp.edu.ar

M. B. Fernández van Raap
e-mail: raap@fisica.unlp.edu.ar

A. Veiga
e-mail: veiga@fisica.unlp.edu.ar

N. Martínez
e-mail: nmartinez@fisica.unlp.edu.ar

G. A. Pasquevich · P. Mendoza Zélis · F. H. Sánchez · M. B. Fernández van Raap
IFLP, CONICET, La Plata, Argentina

N. Martínez
CICpBA, La Plata, Argentina

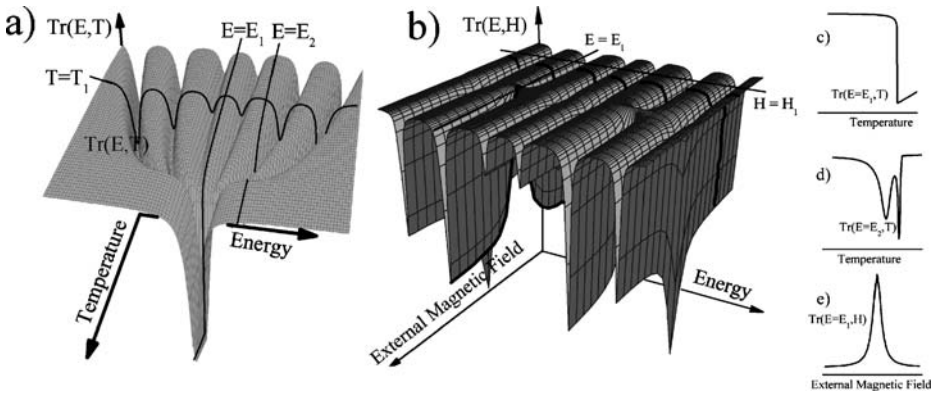

Figure 1 Gamma-ray transmission surface Tr(E, x) for $x = T$ (a) and $x = H$ (b). Intersects with planes E_C = const. correspond to scans (c, d, e). In the two simulated examples, Tr(E_C, x) reflects the hyperfine field-temperature dependence, and the evolution of the average hyperfine field orientation with the intensity of the applied field, respectively.

the measurement of the dynamic response of Fe magnetic moments in nanocrystalline $Fe_{90}Zr_7B_3$ to an external *ac* field.

Key words Mössbauer effect · scans · phase transitions · magnetic response

1 Introduction

Soon after the discovery of the Mössbauer effect, thermal scans performed at a fixed Doppler energy (usually zero energy) were explored in order to rapidly obtain information on magnetic ordering and other characteristic temperatures [1–4]. Nonetheless, to our knowledge, no attempts to formalize this methodology as a fully quantitative analytical tool were carried out until recently [5]. Here, we present experiments which were chosen to demonstrate the usefulness of Mössbauer scans, when they are performed at especially selected photon energies and appropriately combined with Mössbauer spectroscopy. They include the studies of the temperature dependence of the Fe hyperfine magnetic fields in $FeSn_2$ and Fe_3Si, of the thermal evolution and the kinetics of nano-crystallization in an amorphous *Finemet*®-precursor alloy, and of the magnetic dynamics in $Fe_{90}Zr_7B_3$ nanocrystalline alloys. In all cases ^{57}Fe 14.4 keV gamma-rays from a ^{57}Co*Rh* source were used.

A common problem in Mössbauer research is the study of resonant gamma ray transmission spectra as a function of temperature T, intensity of an applied field H, time t elapsed since the start of a phase transition or chemical reaction, etc. The information from such experiments can be represented by a gamma-ray transmission surface Tr(E, x), where E is the photon energy relative to the sample, and $x = T$, H, t, etc., (see Figure 1a, b). Intersects of this surface with planes x_C= const. are the spectra, while intersects with planes E_C= const. correspond to scans (Figure 1c, d). In the two simulated examples, Tr(E_C, x) reflects the hyperfine field-temperature dependence, and the evolution of the average hyperfine field orientation with the intensity of the applied field, respectively. The last effect follows from the well known dependence of ^{57}Fe nuclear transition probabilities on the angle between hyperfine field and gamma-ray directions. Scans allow a quasi-continuous study of material properties

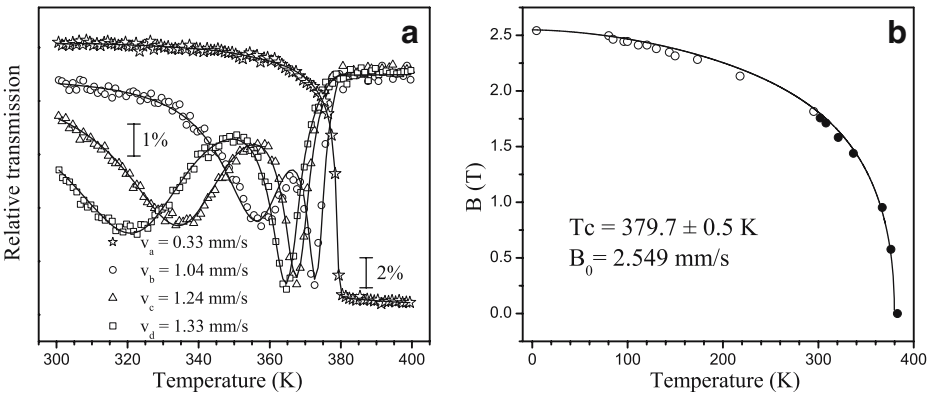

Figure 2 (a) Four scans carried out to determine the quasi-continuous temperature dependence of the Fe hyperfine field $B(T)$ in the antiferromagnet $FeSn_2$. (b) The *solid line* is the $B(T)$ evolution obtained from the simultaneous fit of the results of part (a); *circles* are discrete $B(T)$ values obtained from spectra recorded at fixed temperatures.

dependence upon x and, when time is a limiting factor, may become the only possible Mössbauer approach to study rapidly developing processes.

Saturation effects, even in absorbers nominally thin, influence noticeably the quantitative analysis of scans [5], therefore, the usual thin absorber approximation is not appropriate. For this reason, in order to retrieve information in a reliable quantitative way, the scans were analytically described with the integral expression of the Mössbauer absorption [6].

2 Experiments

As a first experimental example, a set of four scans carried out to determine the quasi-continuous temperature dependence of the Fe hyperfine field $B(T)$ in the antiferromagnet $FeSn_2$ are shown in Figure 2a, [5]. They were recorded at energies which correspond to positions near the spectrum center, and between the room temperature (RT) location of the fourth and fifth spectral lines, using a temperature ramp of 0.125 K/min. The first scan is especially suitable to determine accurately the Nèel temperature T_N, but with the whole set enough information is obtained to deduce the hyperfine field evolution for $T \leq T_N$. In this example, the importance of analyzing the data with the integral expression of the Mössbauer absorption becomes especially clear: saturation effects show a noticeable dependence on temperature, varying very rapidly in the neighbourhood of the Nèel point, where the $FeSn_2$ six lines pattern collapses into a singlet (see Figure 4 of [5]). For their analysis, physical models for the temperature dependence of isomer shift, effective absorber thickness, and the hyperfine field itself were explicitly introduced into the fitting analytic expression [4]. The $B(T)$ evolution obtained from the simultaneous fit of the results of Figure 2a are shown in Figure 2b along with discrete values measured from spectra recorded at fixed temperatures; a remarkable agreement between the two sets of results is observed. A similar approach was used to determine $B(T)$ at each of the two Fe sites of the $D0_3$ structure of ferromagnetic Fe_3Si [7].

Our second example is the thermal evolution of the amorphous ferromagnet $Fe_{73.5}Si_{13.5}Cu_1Nb_3B_9$ (*Finemet*® precursor) and of its nanocrystallisation kinetics [8]. Figure 3a, b show spectra taken at different temperatures and scans recorded between RT and 873 K at an

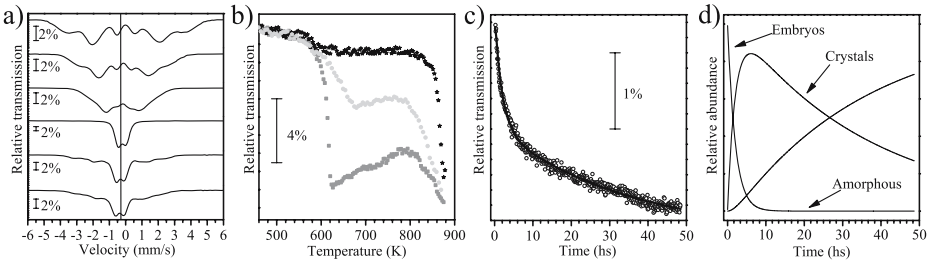

Figure 3 (a) Spectra from amorphous $Fe_{73.5}Si_{13.5}Cu_1Nb_3B_9$ measured at temperatures (*from top to bottom*) of 302, 508, 589, 637, 787, and 803 K. (b) Scans recorded between RT and 873 K at the energy near the spectrum center indicated in (a) by a solid vertical line. (c) Mössbauer transmission vs. time measured during nanocrystallisation at 823 K recorded at a constant energy coincident with one of the principal crystalline absorption lines. (d) Time evolution of the relative amounts of Fe in amorphous phase, crystal embryos and grown up nanocrystals, during nanocrystallisation at 823 K.

energy near the spectrum center (see vertical line in Figure 3a). Scans reflect the different physical processes the material undergoes as temperature increases: ferromagnetic–paramagnetic evolution of the original amorphous phase, nanocrystallisation, and ferromagnetic–paramagnetic evolution of the crystalline Fe–Si nanoparticles. The successive scans performed by heating and cooling back and forth the sample at constant rates of 2 K/min reveal changes in the relative fractions of Fe in amorphous and crystalline environments and a consequent modification of the amorphous phase composition and Curie temperature. The kinetics of nanocrystallisation was observed at 823 K recording the Mössbauer transmission as a function of time at a constant energy coincident with one of the most prominent crystalline absorption lines (Figure 3). The time evolution of the relative amounts of Fe in amorphous phase, crystal embryos and grown up nanocrystals was obtained (Figure 3c) using the hyperfine parameters of each component, obtained from a few Mössbauer spectra. It is worth mentioning that a real time determination of such evolution by Mössbauer spectroscopy is not possible at 823 K (though it can be done at lower temperatures, see Fig. 6 of [8]) because crystallization occurs too rapidly to allow recording of a good quality spectrum representative of a given intermediate state of transformation.

As a final example we present, for the first time, an on going experiment designed to study the dynamic response to an applied *ac* field, of Fe magnetic moments at different phases of $Fe_{90}Zr_7B_3$ ribbons in the nanocrystalline state. In this state, 15–20 nm Fe(Zr) crystals (nanocrystalline phase), which occupy 80–85% of the materials volume, are embedded in an amorphous Fe–Zr–B phase. A sketch of the experimental setup is shown in Figure 4. A triangular waveform was used to drive the current through the Helmohltz coils and to address the recording of the Mössbauer transmission to successive channels of a multi scaler. The Helmholtz coils provide an oscillating magnetic field parallel to the ribbon surface with a maximum intensity of about 75 Oe. For the preliminary experiments presented here the field was driven at 10^{-3} Hz. This low frequency enables a direct comparison between scans and spectra, which is important to test this new experimental approach. An investigation of the magnetic scan-frequency dependence in this material is currently on the way. To obtain information on the responses of the nanocrystalline and amorphous phases, data was recorded at two fixed photon energies where the relative absorption from both phases is different. The arrows in Figure 5a indicate these fixed energies E_i (i=5 and 6) and Figure 5b, c, show the results $Tr_i = Tr(E_i,H)$, which exhibit quite different H-dependences for i=5 and 6. Tr_6, where almost only the nanocrystalline contributions (both from crystals interior and surface) should

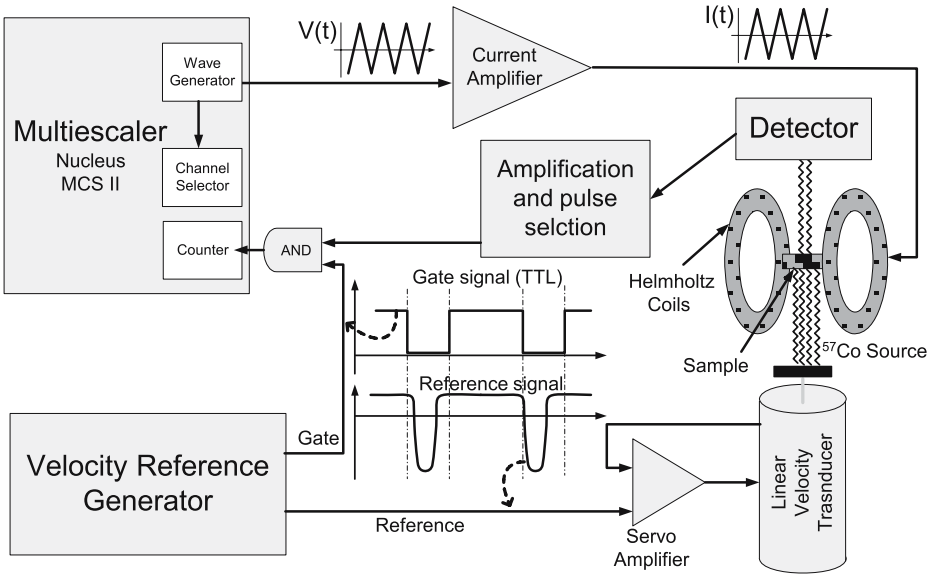

Figure 4 Sketch of the experimental setup for magnetic scans.

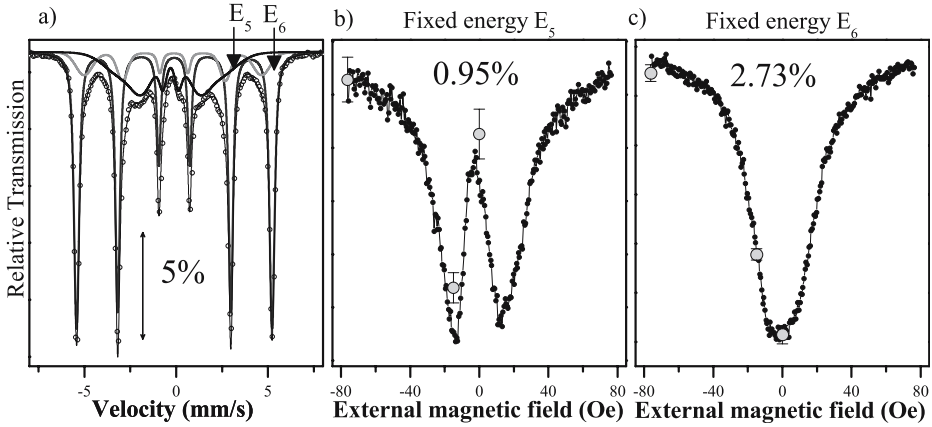

Figure 5 (a) Mossbauer spectrum of amorphous $Fe_{90}Zr_7B_9$ recorded for H=0, showing the contributions from nanocrystals interior (sextet with larger and sharper absorption lines), nanocrystals surface (intermediate average hyperfine field sextet) and amorphous phase. (b) and (c) Mössbauer transmission $Tr_I = Tr(E_i,H)$ as a function of applied field H recorded at the fixed energies E_i (i=5 and 6) indicated by *arrows* in (a). *Full circles* are $Tr(E_i,H)$ obtained from Mössbauer spectra taken at the corresponding fields.

be present [9], has the expected qualitative behaviour, i.e., an increase of transmission with increasing intensity of the applied field, with a tendency for saturation at high fields (see also Figure 1d). Tr_5, instead, has a complex behaviour. Opposite contributions from nanocrystals (fifth lines from crystals interior and surface) and amorphous (sixth line) are expected here, because transition intensities corresponding to lines five and six have opposite dependences on the hyperfine field direction. However, taking into account the amorphous relative amount, its effect would be too small as to justify the observed pattern at that energy. This

complex behaviour could be related to polarization effects which appear in thick absorbers [10]. To confirm this behaviour, a few spectra were recorded under external fields (H_j=−70.6, −15.3 and 0 Oe). In Figure 5b,c, the full circles are the values Tr(E_5,H_j) and Tr(E_6,H_j), respectively obtained from the spectra, and they agree with the behaviour revealed by the scan. The analysis of the physics beneath these results is left for a forthcoming article, but we found worthily to remark that its observation was possible by performing only one scan at energy E_5.

3 Conclusion

In conclusion, we have proved here, that the Mössbauer effect thermal and magnetic scans constitute a powerful tool, complementary of Mössbauer spectroscopy, for studying a variety of condensed matter phenomena. We are currently carrying out new developments of scans. Magnetic scans can be readily extended up to frequencies of 10^3–10^4 Hz, and applied *ac* fields can be substantially increased. Using velocity waveforms especially designed, and/or feedback mechanisms to vary velocity parameters based of the instantaneous outcome of an ongoing experiment, the applications of scans can be largely extended.

Acknowledgements We wish to acknowledge Prof. Teruo Bitoh for kindly providing us with the high quality $Fe_{90}Zr_7B_3$ amorphous ribbons and Prof. Elisa Baggio Saitovitch for kindly allowing one of us (G.A.P.) to use a high vacuum–high temperature device to perform the nanocrystallization of these ribbons. We are also grateful for encouraging discussions of G.A.P. with Profs. Bitoh and Baggio-Saitovich. This work has been done under financial support from CONICET and UNLP.

References

1. Preston, R.S., Hanna, S.S., Heberle, J.: Phys. Rev. **128**, 2207 (1962)
2. Gonser, U., Meechan, C.J., Muir, A.H., Wiedersich, H.: J. Appl. Phys. **34**, 2373 (1963)
3. Wagner, H.-J., Gonser, U.: J. Magn. Magn. Mater. **31–34**, 1343 (1983)
4. Chien, C.L.: Phys. Rev., B. **18**, 1003 (1978)
5. Mendoza Zélis, P., Pasquevich, G.A., Sánchez, F.H., Martínez, N., Veiga A.: Phys. Lett., A. **298**, 55 (2002)
6. Vèrtez, A., Korecz, L., Burger, K., In: Mössbauer Spectroscopy and Transition Metal Chemistry, p.31. Elsevier, Ámsterdam (1979)
7. Pasquevich, G.A., Mendoza Zélis, P., Fernández van Raap, M.B., Sánchez, F.H.: Physica. B **354**, 369 (2004)
8. Sánchez, F.H., Pasquevich, G.A., Mendoza Zélis, P., Cabrera, A.F., Ying-feng, L., Vázquez, M.: J. Metastable Nanocryst. Mater. **22**, 39 (2004)
9. Miglierini, M., Greneche, J.M.: J. Phys.: Condens. Matter **9**, 2321 (1997)
10. Williams, J.M., Brooks, J.S.: Nucl. Instrum. Methods **128**, 363 (1975)